Hong Kong J Radiol. 2020;23:50-6 | https://doi.org/10.12809/hkjr2017055

PICTORIAL ESSAY

Familial Haemophagocytic Lymphohistiocytosis: Spectrum of Neuroimaging Findings in Three Siblings

BYW Li, TW Yeung, HY Lau

Department of Radiology, Tuen Mun Hospital, Tuen Mun, Hong Kong

BACKGROUND FAMILY HISTORY

A consanguineous Pakistani couple presented with a history of recurrent miscarriages and infant deaths (Figure 1). Their first pregnancy ended with intrauterine death at 27 weeks of gestation. The second pregnancy produced twins: twin I died at age 18 months and twin II was male and currently healthy with normal development. The third pregnancy produced a male who presented with status epilepticus and global developmental delay at age 2 years. He developed persistent breakthrough seizures despite being prescribed long-term anticonvulsants and died at age 34 months after developing multiorgan failure. The fourth pregnancy ended with miscarriage at 8 weeks of gestation. The fifth pregnancy produced a female who was clinically followed up from birth due to a family history of suspected neurodegenerative disease. This girl was found to have developmental delay at age 12 months and became epileptic. She was subsequently diagnosed with familial haemophagocytic lymphohistiocytosis (fHLH) following whole exome sequencing that detected a homozygous missense mutation in the *PRF1* (perforin) gene. Post-mortem genetic sequencing subsequently identified the same mutation in the deceased elder brother from the third pregnancy.

IMAGING FINDINGS

The computed tomography and magnetic resonance imaging (MRI) brain findings of the three affected siblings are reviewed, two of whom were diagnosed with fHLH and the third who died of suspected complications of the same disease. A review of the imaging findings for the three patients is summarised in the Table.

Patient 1

The first affected sibling was twin I from the second pregnancy who was born at term following an unremarkable perinatal history. He presented with signs and symptoms of neurodegeneration at age 5 months. Laboratory investigations revealed a salient finding of elevated serum neopterin and immunoglobulin G.

The initial MRI scan showed an infiltrative heterogeneous high-intensity T1 signal involving bilateral deep grey matter (basal ganglia, thalamus), bilateral cerebral (corona radiata, centrum semiovale) and cerebellar white matter and brainstem (midbrain and pons).

Differentials at that time included malignancy such as malignant brainstem glioma, primitive neuroectodermal tumours, and atypical rhabdoid teratoid tumour.

Correspondence: *Dr BYW Li, Department of Radiology, Tuen Mun Hospital, Tuen Mun, Hong Kong*
Email: birgittali@gmail.com

Submitted: 20 Nov 2018; Accepted: 31 Dec 2018.

Contributors: All authors contributed to the concept of study, acquisition and analysis of data, drafting of the manuscript, and had critical revision of the manuscript for important intellectual content. All authors had full access to the data, contributed to the study, approved the final version for publication, and take responsibility for its accuracy and integrity.

Conflicts of Interest: All authors have disclosed no conflicts of interest.

Funding/Support: This pictorial essay received no specific grant from any funding agency in the public, commercial, or not-for-profit sectors.

Ethics Approval: This study was approved by the New Territories West Cluster Research Ethics Committee (Ref NTWC/REC/20001).

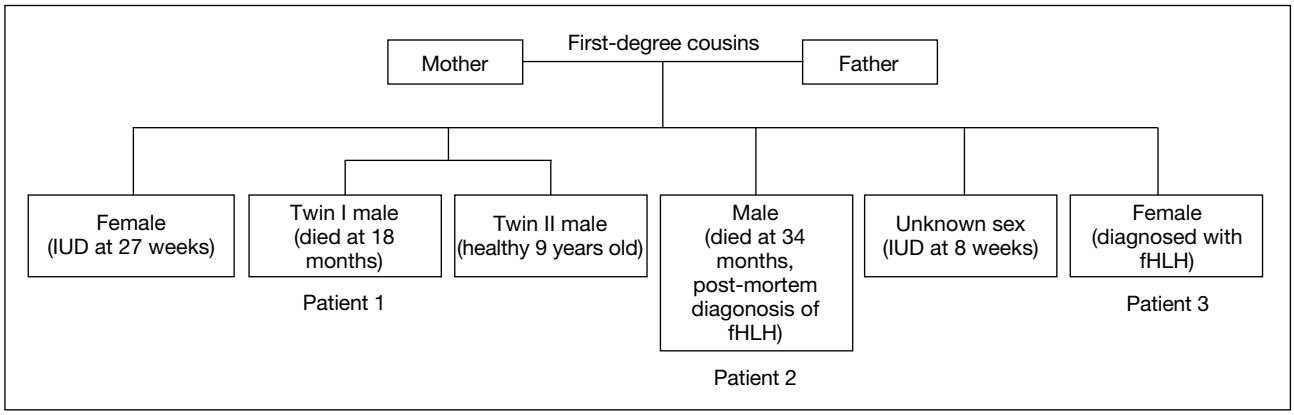

Figure 1. Pedigree chart of the family.
Abbreviations: fHLH = familial haemophagocytic lymphohistiocytosis; IUD = intrauterine death.

Table. Summary of clinical, laboratory and neuroradiological findings in the three siblings

	Patient 1	Patient 2	Patient 3
Age at onset	5 months	16 months	12 months
Presenting symptoms	Neurodegeneration	Developmental regression	Developmental regression
Progression of symptoms	Seizures	Status epilepticus at 23 months	Status epilepticus at 12 months
Magnetic resonance imaging findings	Mixed solid-cystic lesions in cerebrum and cerebellum	Enhancing cerebellar lesion Leptomeningeal enhancement	Abnormal gyral and subcortical white matter signal in cerebrum and cerebellum Abnormal MR spectroscopy (decreased choline, creatine and N-acetyl aspartate)
Laboratory findings	Raised CSF IgG, neopterin	Raised serum IgG, ferritin Reduced serum fibrinogen Raised CSF IgG, neopterin Homozygous missense mutation in *PRF1* gene	Raised CSF IgG Low serum NK cells Homozygous missense mutation in *PRF1* gene
Outcome	Death at 18 months due to chest infection	Death at 34 months due to multi-organ failure	Long-term hospitalisation with frequent breakthrough seizures

Abbreviations: CSF = cerebrospinal fluid; IgG = immunoglobulin G; MR = magnetic resonance.

Computed tomography brain studies demonstrated progressive increase in bilateral cortical and thalamic calcifications (Figure 2).

Subsequent MRI scan a month later showed enlargement of the high-intensity T1 signal lesion in bilateral deep grey matter, cerebral white matter and brainstem (Figure 3a), and an extensive high-intensity T2 signal in bilateral cerebral white matter and blooming artefacts suggestive of calcifications and haemosiderin deposition (Figure 3b and c).

Patient 2

The second case was the male child from the third pregnancy who developed developmental regression at age 16 months and was admitted to hospital at age 23 months after presenting with status epilepticus. Abnormal laboratory tests showed elevated levels of immunoglobulin G and neopterin in the cerebrospinal fluid (CSF). Elevated ferritin, triglyceride, immunoglobulin G and reduced fibrinogen blood serum levels were also evident. Post-mortem exome sequencing of the patient's DNA revealed a *PRF1* genetic mutation.

Initial MRI brain showed restricted diffusion at the deep cortical region of the cerebrum suggestive of hypoxic ischaemic brain insult. There was also a rim-enhancing right cerebellar lesion. An infective or inflammatory process or neoplasm was initially considered.

Serial brain MRI scans showed interval enlargement of the right cerebellar lesion (Figure 4c) and increasing high-intensity T2 signal in bilateral cerebral and cerebellar white matter as well as bilateral deep grey

nuclei and brainstem (Figure 4a and b). There was also development of diffuse leptomeningeal enhancement (Figure 4d).

Patient 3

The female child from the fifth pregnancy presented with convulsions and status epilepticus at age 12 months.

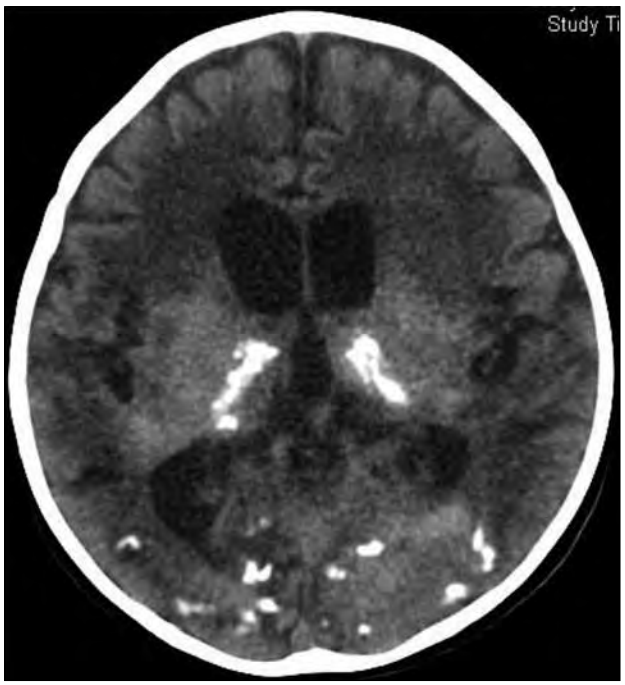

Figure 2. Computed tomography scan showing bilateral cortical and thalamic calcifications in patient 1.

Elevated serum immunoglobulin G was detected. Subsequently, whole exome sequencing detected a homozygous missense mutation at the *PRF1* gene.

Initial MRI scan showed patchy confluent high-intensity T2/fluid-attenuated inversion recovery signals along the gyri and subcortical white matter of bilateral cerebral and cerebellar hemispheres (Figure 5a and b). There was also a cluster of tiny enhancing foci at the superior aspect of the cerebellar vermis suspicious of leptomeningeal enhancement (Figure 6). Restricted diffusion was present along the gyri and subcortical white matter of bilateral cerebrum and deep grey matter affecting the thalami and lentiform nuclei (Figure 5c).

Repeat MRI scan after 2 weeks revealed increased high-intensity T2 signal at the deep grey matter, especially at the thalami and lentiform nuclei (Figure 7a), with atrophic changes to the cerebellum. There was partially resolved contrast enhancement at the periphery and edges of the white matter lesions. Previously seen abnormal leptomeningeal enhancement at the superior aspect of the cerebellar vermis also showed partial resolution. However, there was more extensive restricted diffusion along bilateral cerebral gyri and subcortical white matter and new restricted diffusion at bilateral insular cortex and caudate nuclei (Figure 7b and c). Magnetic resonance spectroscopy performed at the same time showed decreased choline, creatine and N-acetyl aspartate at the deep grey nuclei and cerebellar lesions and focal areas of lactate peak.

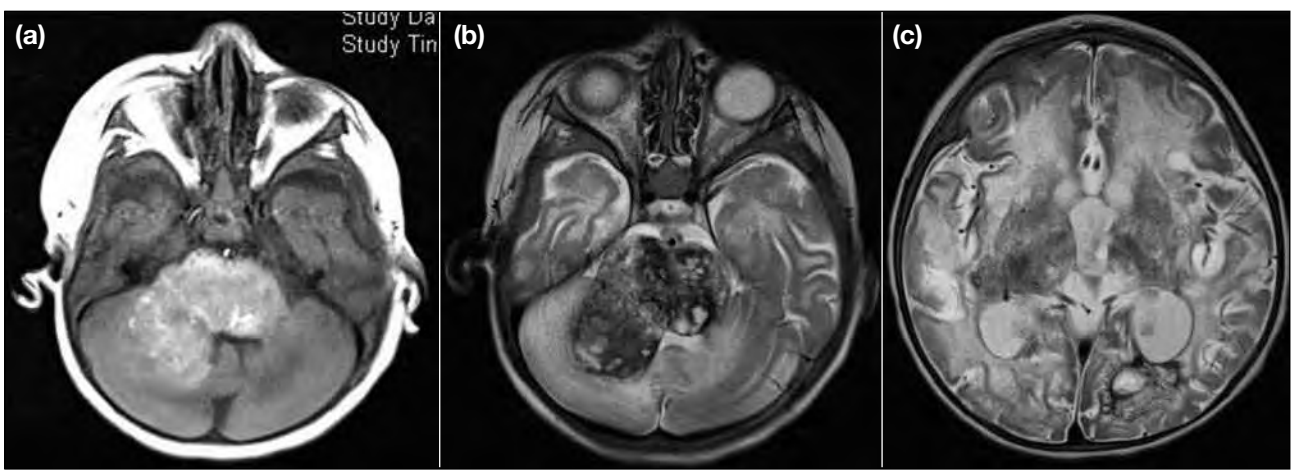

Figure 3. Magnetic resonance imaging scans showing (a) infiltrative intense T1 signal involving the cerebellum, and (b, c) high-intensity T2 signal and blooming in bilateral cerebrum and cerebellum in patient 1.

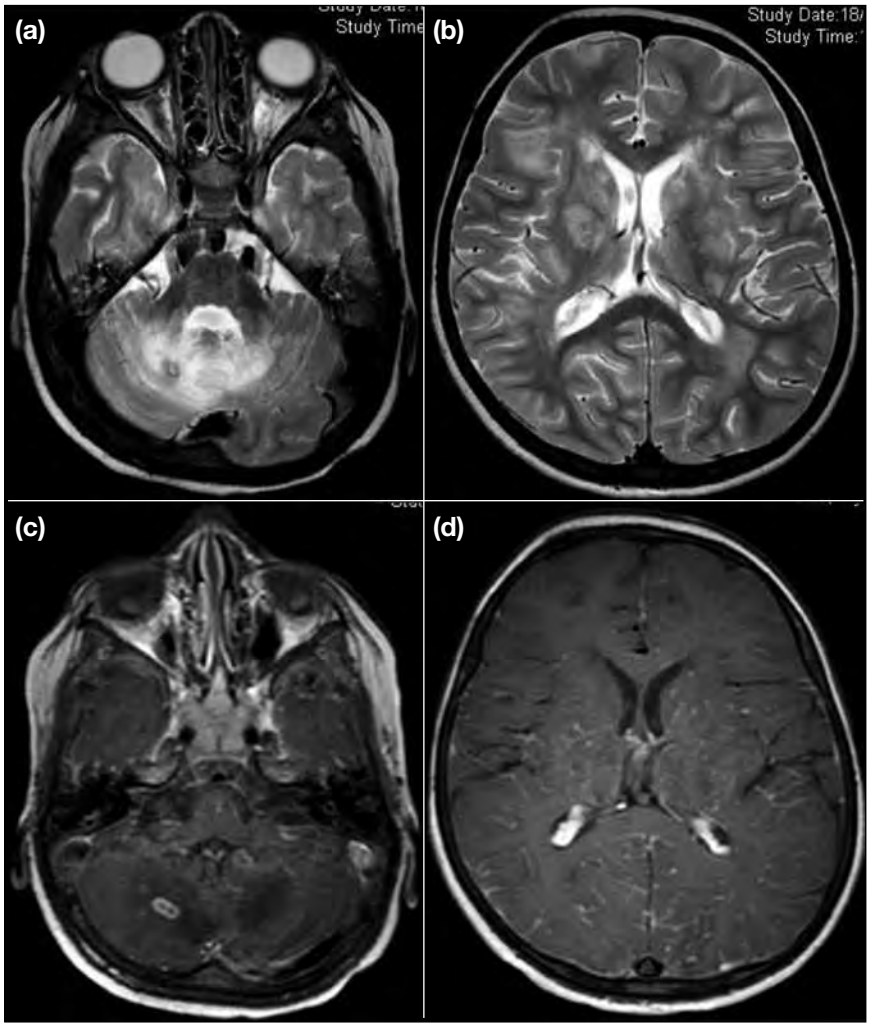

Figure 4. Patient 2. Magnetic resonance imaging scans showing (a, b) high-intensity T2 signal at bilateral cerebral and cerebellar white matter, bilateral deep grey nuclei and brainstem; (c) right cerebellar rim-enhancing lesion; and (d) diffuse leptomeningeal enhancement affecting both supra- and infra-tentorial regions.

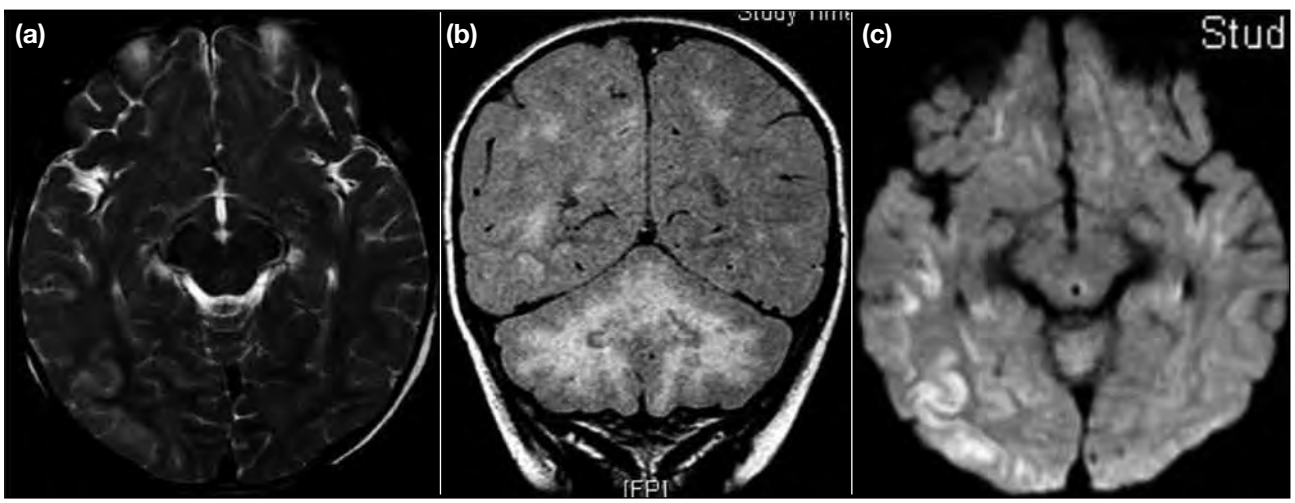

Figure 5. Patient 3. Magnetic resonance imaging scans showing (a) T2 and (b) fluid-attenuated inversion recovery high-intensity signals along the gyri and subcortical white matter of bilateral cerebrum and cerebellum; and (c) restricted diffusion along gyri and subcortical white matter of bilateral cerebrum and deep grey matter.

The MRI scan performed 1 month later showed progressive brain parenchymal loss with extensive white matter high-intensity T2 signal, also involving the lentiform nuclei and cerebellum (Figure 8). Progressive ventriculomegaly was also observed, compatible with generalised brain parenchymal atrophy.

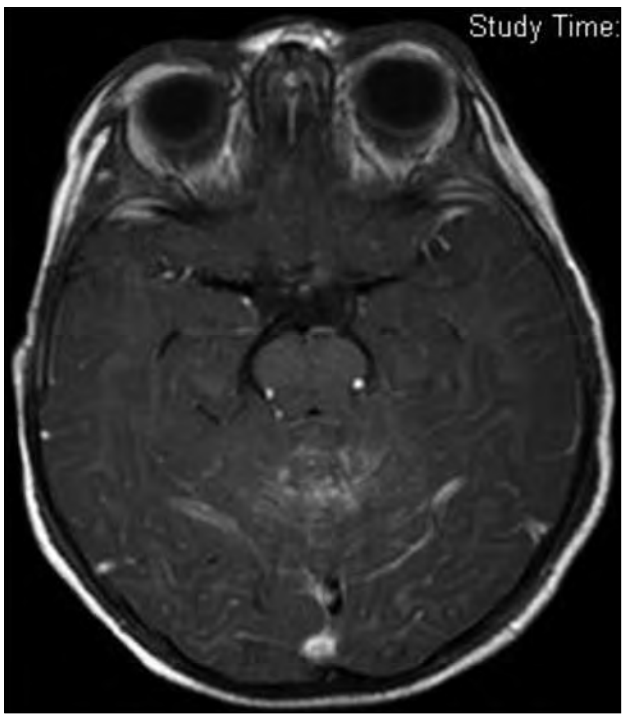

Figure 6. Patient 3. Magnetic resonance imaging scan showing leptomeningeal enhancement at the superior aspect of the cerebellar vermis.

DISCUSSION

HLH is a progressively fatal disease characterised by uncontrolled proliferation of activated, non-neoplastic lymphocytes and macrophages, resulting in phagocytosis of other blood cells and overproduction of inflammatory cytokines. It can be divided into primary and secondary forms. The primary (familial) form of HLH (as in our case series) is related to genetic abnormalities with an autosomal recessive mode of inheritance and is usually diagnosed in the first 2 years of life. The secondary form is associated with infection, malignancy, and prolonged immunosuppression.

The clinical and neuroradiological findings are indistinguishable between the two forms of HLH and most clinical episodes in the familial form are triggered by infection. Therefore, any underlying infection or causative agent should be sought even when suspecting fHLH.

The diagnosis of HLH is based on established clinical and laboratory diagnostic criteria, including family history, fever, splenomegaly, cytopenia of at least two cell lines, hypertriglyceridaemia, hypofibrinogenaemia, elevated ferritin, histological evidence of haemophagocytosis in the bone marrow, CSF, or lymph nodes and detection of genetic mutations.[1] The neuroradiological findings are supportive but not sufficiently specific to achieve the diagnosis.

It is known that the clinical outcome of HLH is poor, particularly if untreated, but the introduction of specific

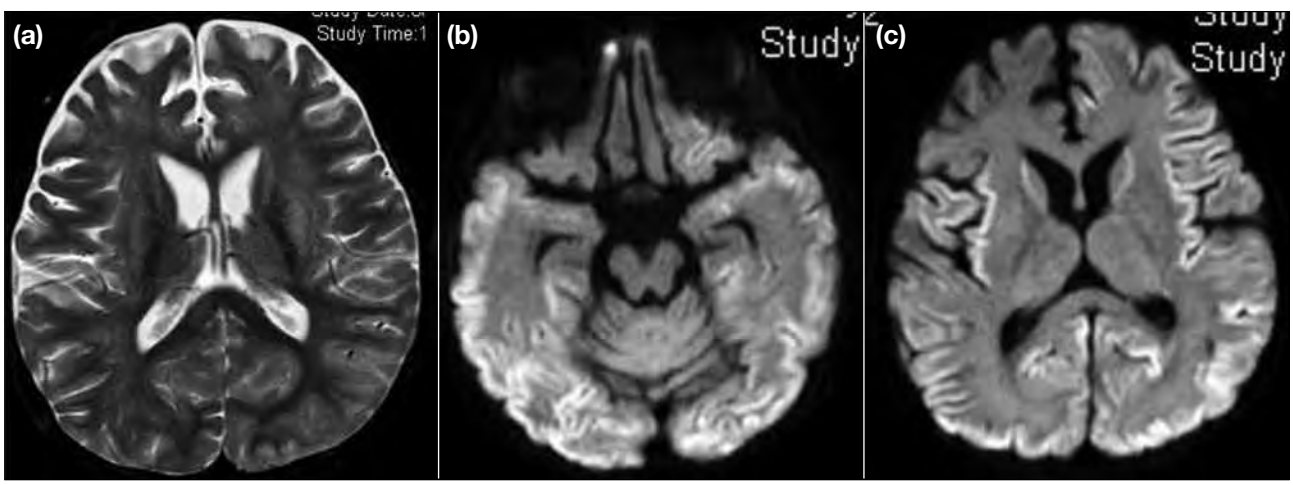

Figure 7. Patient 3. Magnetic resonance imaging scans showing (a) high-intense T2 signal at the deep grey matter; and (b, c) extensive restricted diffusion along bilateral cerebral gyri and subcortical white matter and at bilateral insular cortex and caudate nuclei.

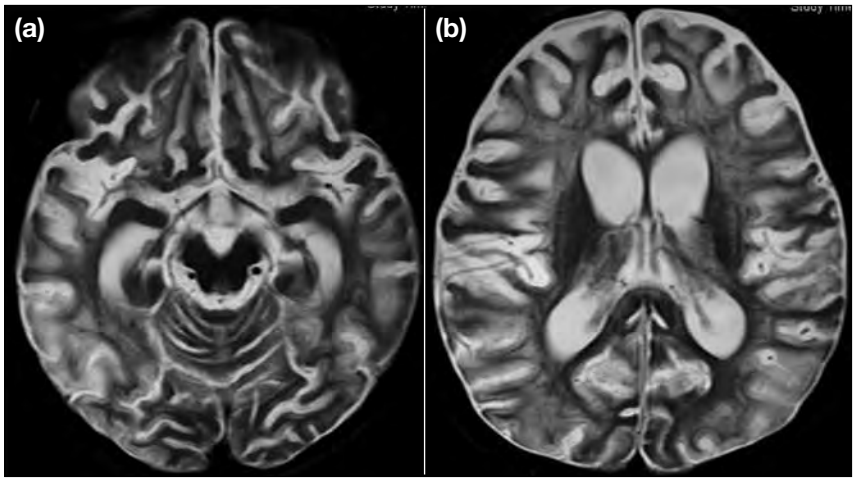

Figure 8. Patient 3. (a, b) Magnetic resonance imaging scans showing progressive atrophy of brain parenchyma with extensive white matter high-intensity T2 signal.

treatment protocols (HLH-94 and HLH-2004) has improved the prognosis. More recently, stem cell or bone marrow transplantation has become a promising treatment option for patients with primary HLH.[2]

In addition to sepsis and haemorrhage, central nervous system (CNS) involvement is another main contributor to morbidity and mortality in HLH. CNS involvement is frequent and often progressive but can be treated. Therefore, the importance of early detection, accurate evaluation of severity, and monitoring of treatment response with neuroimaging studies cannot be stressed enough.

Depending on the patient's clinical presentation and neuroimaging findings, other differential diagnoses may have to be considered, including brain abscess, metastasis, multiple sclerosis, acute disseminating encephalomyelitis, lymphoma, malignant glioma and even child abuse.

In paediatric patients with CNS involvement, the histopathological findings can be classified by the microscopic stages of disease, as characterised by increasing severity[3,4]: stage I shows leptomeningeal lymphocyte and histiocyte infiltration; stage II represents additional parenchymal involvement with perivascular infiltration; and stage III progresses to cerebral tissue necrosis, gliosis and demyelination in addition to massive tissue infiltration most significantly affecting the white matter.

A correlation between the histopathological stage and CNS imaging findings has been described.[3-5] CNS infiltration typically begins in the meninges, and then induces perivascular changes.[6] Radiographically, stage I is represented by leptomeningeal enhancement, as seen on the initial MRI in one of our patients (Figure 6). The extent of enhancement in HLH likely correlates with the degree of meningeal infiltration by lymphocytes and histiocytes. In previous studies, leptomeningeal contrast enhancement has also been shown to correlate with clinical symptoms of meningitis.[4]

Imaging findings for stages II and III include diffuse white matter changes with variable enhancement, haemorrhage and restricted diffusion, progressing to parenchymal infarction, calcifications, and atrophy. Other imaging findings include delayed myelination, hydrocephalus, and subdural fluid collections.[3,4] Our patients presented with a wide spectrum of imaging findings encompassing different stages.

Enhancing parenchymal lesions have been described in HLH with CNS involvement, and predominantly affect the cerebrum and cerebellum.[7-9] In one of our cases, a large right cerebellar enhancing lesion was shown on MRI. Additionally, nodular or ring-enhancing brain parenchymal lesions have been reported,[9,10] as seen in one of our patients (Figure 4c) and is postulated to be due to the compromised blood-brain barrier associated with active demyelination.

Ventriculomegaly identified in patients with CNS involvement in HLH may be due to communicating hydrocephalus or parenchymal atrophy. In two of our cases, progressive ventricular enlargement and widening of the sulcal spaces was likely due to parenchymal

atrophy. In cases of communicating hydrocephalus, the underlying cause may be a disturbance in CSF drainage due to leptomeningeal infiltration.

Assessment of restricted diffusion on diffusion-weighted imaging sequence is useful in cases of HLH. Restricted diffusion in white matter lesions in HLH is well reported in the literature,[8] and it was also evident in one of our patients. This is postulated to be due to neuronal loss along with cytotoxic oedema and demyelination in the acute phase of the disease.[3]

Magnetic resonance spectroscopy performed in one of our patients also showed metabolic changes correlating with neuroimaging findings, with markedly reduced choline, creatine, and N-acetyl aspartate suggesting decreased neural density and gliosis representing the end result of tissue destruction.[9] Focal areas of lactate peak were suggestive of anaerobic metabolism.

Overall, the severity of CNS involvement in HLH is variable and related to the duration of illness. The neuroimaging findings correlate with clinical evolution and are useful to monitor disease progression or regression. Imaging findings should be correlated with clinical symptoms in addition to laboratory and pathological findings in order to narrow the differential diagnosis and provide timely diagnosis of patients with HLH.

CONCLUSION

fHLH is a rare hereditary disease and can present with a wide range of neuroradiological findings. Despite the typically non-specific clinical presentation, awareness of this entity and familiarity with the spectrum of imaging findings may facilitate early diagnosis and timely commencement of appropriate treatment to modify and improve the disease course.

REFERENCES

1. Janka GE. Familial and acquired hemophagocytic lymphohistiocytosis. Eur J Pediatr. 2007;166:95-109. Crossref
2. Hallahan AR, Carpenter PA, O'Gorman-Hughes DW, Vowels MR, Marshall GM. Hemophagocytic lymphohistiocytosis in children. J Paediatr Child Health. 1999;35:55-9. Crossref
3. Chung TW. CNS involvement in hemophagocytic lymphohistiocytosis: CT and MR findings. Korean J Radiol. 2007;8:78-81. Crossref
4. Anderson TL, Carr CM, Kaufmann TJ. Central nervous system imaging findings of hemophagocytic syndrome. Clin Imaging. 2015;39:1090-4. Crossref
5. Rooms L, Fitzgerald N, McClain KL. Hemophagocytic lymphohistiocytosis masquerading as child abuse: presentation of three cases and review of central nervous system findings in hemophagocytic lymphohistiocytosis. Pediatrics. 2003;111(5 Pt 1):e636-40. Crossref
6. Kim MM, Yum MS, Choi HW, Ko TS, Im HJ, Seo JJ, et al. Central nervous system (CNS) involvement is a critical prognostic factor for hemophagocytic lymphohistiocytosis. Korean J Hematol. 2012;47:273-80. Crossref
7. Shinoda J, Murase S, Takenaka K, Sakai N. Isolated central nervous system hemophagocytic lymphohistiocytosis: case report. Neurosurgery. 2005;56:E187-90. Crossref
8. Ozgen B, Karli-Oguz K, Sarikaya B, Tavil B, Gurgey A. Diffusion-weighted cranial MR imaging findings in a patient with hemophagocytic syndrome. AJNR Am J Neuroradiol. 2006;27:1312-4.
9. Goo HW, Weon YC. A spectrum of neuroradiological findings in children with haemophagocytic lymphohistiocytosis. Pediatr Radiol. 2007;37:1110-7. Crossref
10. Akima M, Sumi SM. Neuropathology of familial erythrocytic lymphohistiocytosis: six cases and review of the literature. Hum Pathol. 1984;15:161-8. Crossref